MICROSTRUCTURAL EFFECTS ON THE CLEAVAGE FRACTURE STRESS IN FULLY PEARLITIC 1080 STEEL

J. J. Lewandowski* and A. W. Thompson**

*Department of Metallurgy and Materials Science, University of Cambridge, Pembroke Street, Cambridge CB2 3QZ, England

**Department of Metallurgical Engineering and Materials Science, Carnegie-Mellon University, Pittsburgh, PA 15213, USA

ABSTRACT

Blunt-notched bend bars of fully pearlitic AISI 1080 steel were tested in four-point bending at temperatures ranging from room temperature down to -125°C to determine the influence of microstructural parameters on the critical cleavage fracture stress. The cleavage fracture stress, σ_F, decreased with increasing pearlite interlamellar spacing and was independent of the prior austenite grain size. Specimens possessing fine pearlitic microstructures exhibited temperature independent values for σ_F and provided both metallographic and fractographic evidence of sub-notch fracture initiation. While these observations are consistent with propagation-controlled cleavage, the location of the sub-notch cracks as well as their morphology with respect to the microstructure indicated that fracture initiation occurred by a strain-assisted process.

KEYWORDS

Cleavage fracture stress; sub-notch microcracks; pearlitic microstructures

INTRODUCTION

Cleavage Fracture Theories

Orowan's (1945) theory of brittle fracture was one of the earliest attempts at explaining cleavage fracture, where it was postulated that a critical value of tensile stress was required to produce cleavage. Furthermore, this "brittle fracture stress" was assumed to be relatively independent of temperature. Subsequent experiments on notched specimens of mild steel fractured prior to general yield supported such an argument (Hendrickson, Wood, and Clark, 1958; Knott, 1966a), and further indicated that some degree of localized flow or plasticity was required to initiate cleavage fracture in mild steels. Recognizing that brittle fracture required some degree of localized plasticity prompted a number of dislocation models for slip-initiated cleavage fracture (Cottrell, 1958; Stroh, 1954). However, the observation that coarse carbides promoted brittle fracture in steels (McMahon and Cohen, 1965) required the inclusion of microstructural parameters into any predictive model. Consequently, subsequent models (Lindley, Oates, and Richards, 1970; Smith, 1966) incorporated microstructural parameters such as the grain size and carbide thickness.

The typical method of determining the cleavage fracture stress involves fracturing blunt-notched bend specimens over a range of test temperatures and subsequently calculating the sub-notch stresses at fracture with the aid of an appropriate stress analysis. Before finite-element techniques were available for determining the distribution and magnitude of stresses in notched specimens, stress analyses were based on slip-line field theory (Green and Hundy, 1956) which modelled the material as behaving in a rigid-perfectly plastic manner (i.e. zero work-hardening). However, finite-element stress analysis of a notched bend specimen (Griffiths and Owen, 1971) has shown that the inclusion of moderate linear work-hardening (e.g. E/120, where E = Young's Modulus) changes both the distribution and magnitude of the stresses in the notched bar in comparison to values predicted by slip-line field theory. Although much of the early experimental work on cleavage fracture focussed on mild steels, recent work has investigated microstructural effects on the cleavage fracture stress in martensitic (Kõtilainen, 1980), bainitic (Curry, 1982; Kõtilainen, 1980), and spheroidized steels (Curry and Knott, 1978) of various compositions. The present work was intended to investigate microstructural effects on the cleavage fracture stress in fully pearlitic microstructures, and was part of a larger study of hydrogen effects on cleavage fracture (Lewandowski, 1983; Lewandowski and Thompson, 1984).

Deformation and Fracture of Fully Pearlitic Microstructures

Eutectoid steels may be heat treated to provide independent variation of the pearlite interlamellar spacing and the prior austenite grain size (Hyzak and Bernstein, 1976). The pearlite interlamellar spacing controls the yielding and deformation behaviour in these microstructures (Hyzak and Bernstein, 1976; Porter, Easterling, and Smith, 1978), where the yield stress varies inversely with interlamellar spacing. A proposed dislocation model (Miller and Smith, 1970) for shear cracking of pearlitic microstructures is illustrated in Fig. 1. Coarse pearlitic microstructures possess low strength and initially deform by dislocation generation at ferrite/cementite interfaces (Burns and Pickering, 1964). As deformation proceeds, slip localizes into slip bands which create offsets in the cementite (Pepe, 1973; Porter, Easterling, and Smith, 1978), thereby acting as local stress concentrators which increase the fiber loading stresses in the lamellae. Fracture of the cementite ensues, Fig. 1a, creating an easy path for further deformation. Intense shear in the adjoining ferrite follows, Fig. 1b, fracturing adjacent cementite lamellae. Eventually, voids form in the ferrite at the end of the cementite lamellae, Figs. 1c and 1d. The local stresses are subsequently elevated during void growth, eventually producing rapid brittle failure.

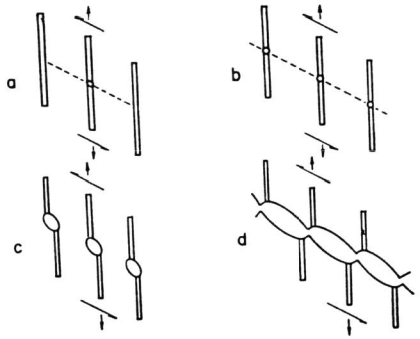

Fig. 1. Dislocation model (Miller and Smith, 1970) of shear cracking in pearlitic microstructures.

Fine pearlitic structures, on the other hand, possess higher strength and deform in a more homogeneous manner (Miller and Smith, 1970; Porter, Easterling, and Smith, 1978). Slip is more homogeneously distributed in the form of less intense, but more closely spaced, slip bands. The fine cementite lamellae also appear to behave in a more ductile manner, as they may rupture by necking rather than failing in a brittle manner (Miller and Smith, 1970; Langford, 1977). Void growth and coalescence is again interrupted by cleavage.

While the interlamellar spacing controls the yielding behaviour in these microstructures, the prior austenite grain size controls the Charpy impact toughness for an equivalent pearlite spacing (Hyzak and Bernstein, 1976). Park and Bernstein (1979) later showed that Charpy impact toughness in pearlitic microstructures was controlled by an effective grain size which was essentially the prior austenite grain size. Apparently, the ferrite in pearlite colonies nucleated from the same austenite grain boundary exhibit a common {100} orientation (Park and Bernstein, 1979), enabling cleavage fracture across similarly oriented ferrite in those colonies. A larger prior austenite grain size increases the size of these "cleavage fracture units", thereby reducing the Charpy impact toughness. While this explanation is consistent with the trends exhibited in impact testing of these microstructures, plane strain toughness values (i.e. K_{IC}) do not exhibit a similar microstructure dependence (Alexander, 1983).

The goal of the present work was to determine the microstructural parameters controlling the cleavage fracture stress, σ_F, in fully pearlitic microstructures. Independent variation of the prior austenite grain size and the pearlite interlamellar spacing provided the microstructure test matrix, while blunt-notched bend bars were tested to determine σ_F. In addition, the present work was intended to focus on crack initiation phenomena.

EXPERIMENTAL PROCEDURE

The chemical composition of the steel used in the present work was analyzed to be, in weight percent: 0.81 Carbon; 0.85 Manganese; 0.02 Sulphur; 0.018 Phosphorus; balance Iron, conforming to the specifications for AISI 1080 steel. Specimen blanks were heat treated prior to machining. Austenitization was conducted in dry argon at either 1000°C/3 hr. or 800°C/1 hr., followed by isothermal transformation in molten lead maintained at either 675°C or 550°C. These heat treatments produced combinations of either a coarse (designated CG) or fine (i.e. FG) prior austenite grain size with either a coarse (i.e. CS) or fine (i.e. FS) interlamellar spacing. Table 1 lists the heat treatments employed and their effect on the microstructural parameters of interest to the present work.

TABLE 1 Heat Treatments and Resultant Microstructures

Heat Treatment (microstructure)	Austenite Grain size (μm) ± 5μm	Pearlite Colony size (μm) ± 1μm	Pearlite Spacing (μm)
1000°C/3 hr., 550°C/45 min. (CG/FS)	170	6.5	0.11
800°C/1 hr., 550°C/45 min. (FG/FS)	30	5.5	0.125
1000°C/3 hr., 675°C/45 min. (CG/CS)	170	6.0	0.25
800°C/1 hr., 675°C/45 min. (FG/CS)	30	6.0	0.29

Tensile properties were obtained on ASTM E8 cylindrical tensile specimens tested at temperatures of: 23°C; -25°C; -75°C; -125°C. All tensile specimens were tested at an initial strain rate of 3.3×10^{-4}/sec.

The four-point bend specimens employed in the present work were dimensionally identical to that of Griffiths and Owen (1971), and are shown in Fig. 2. Both single-notched and double-notched (Knott, 1966b) specimens were tested to failure at constant displacement rates ranging from 0.0063 mm/min to 2.50 mm/min. The bend tests were conducted at the temperatures listed above, while cleavage fracture stresses were calculated with the Griffiths and Owen (1971) finite-element analysis. During testing of the double-notched specimens, usually only one of the notched ligaments would fail. Fracture surfaces of these broken ligaments were examined on a Cambridge Instruments CAMSCAN 4 Scanning Electron Microscope (SEM). However, the unbroken ligament in such specimens represents a specimen unloaded immediately prior to final fracture. These unbroken ligaments were subsequently sectioned parallel to their longitudinal axes and in the direction of crack propagation in an attempt to locate sub-notch cracks. Up to six sections were made on each specimen, with one section positioned at the notch midplane. The longitudinal sections were then metallographically prepared for subsequent examination in the SEM.

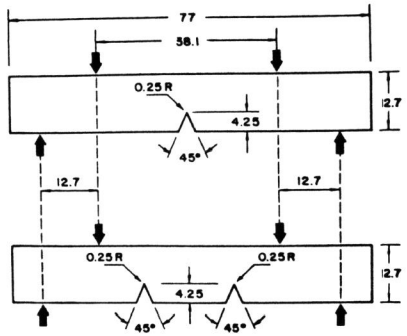

Fig. 2. Single-notched and double-notched bend specimens tested in the present work. Dimensions in mm. Specimen thickness = 12.7 mm.

RESULTS

The heat treatments described in Table 1 produced fully pearlitic microstructures, although specimens transformed at 675°C exhibited approximately 5% area fraction of non-lamellar or "degenerate" pearlite in metallographic sections. Essentially independent variation of the pearlite spacing and the prior austenite grain size was obtained, although specimens austenitized at a higher temperature typically exhibited a finer interlamellar spacing for a given transformation temperature. Table 2 summarizes the temperature and microstructure dependence of the values for the 0.2% offset yield strength and the UTS. Both the yield strength and UTS values were strongly dependent on the interlamellar spacing, consistent with previous results (Hyzak and Bernstein, 1976).

TABLE 2 Temperature Dependence of 0.2% Offset Yield Strength (UTS), MPa

Heat Treatment	+23°C	-25°C	-75°C	-125°C
1000°C/3 hr., 550°C/45 min.	738(1082)	758(1151)	842(1255)	951(1386)
800°C/1 hr., 550°C/45 min.	628(1123)	669(1110)	717(1145)	890(1282)
1000°C/3 hr., 675°C/45 min.	476(917)	524(976)	573(1034)	683(1069)
800°C/1 hr., 675°C/45 min.	386(882)	434(862)	524(903)	628(972)

In the bend tests, fracture was coincident with general yield at room temperature for the two fine pearlitic microstructures. The two coarse pearlitic microstructures exhibited a lower temperature (i.e. -25°C) at which fracture coincided with general yield. The calculated values of the cleavage fracture stress for each microstructure-test temperature combination are summarized in Fig. 3. Neither variations in loading rate nor changes in root radius from 0.25 mm to 0.40 mm significantly changed the calculated values for σ_F (Lewandowski, 1983). Nonetheless, the σ_F data appear to fall into two distinct groups. Bend specimens possessing fine pearlitic microstructures fractured upon attaining a temperature independent value for σ_F. Furthermore, the σ_F values for the two fine pearlitic microstructures scaled with their yield strength ratio at a fixed temperature, and were independent of the prior austenite grain size. The coarse pearlitic specimens, on the other hand, exhibited temperature dependent values for σ_F over a slightly reduced range of test temperatures.

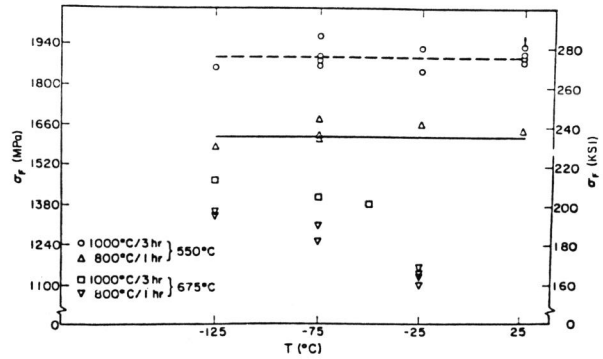

Fig. 3. Calculated values for σ_F.

Fracture surfaces of the fine pearlitic bend specimens were typically 100% cleavage, as shown in Fig. 4. However, examination of the notch root regions at low magnification (e.g. 100-200X) revealed what appeared to be sub-notch fracture initiation sites. Cleavage river lines emanating both toward the notch as well as away from it originated at sub-notch root cleavage facets, as illustrated in Fig. 4. These features were observed for all microstructure-test temperature combinations and are possibly indicative of precusors to final fracture. Cleavage regions in all specimens exhibited facet sizes which correlated with the prior austenite grain size.

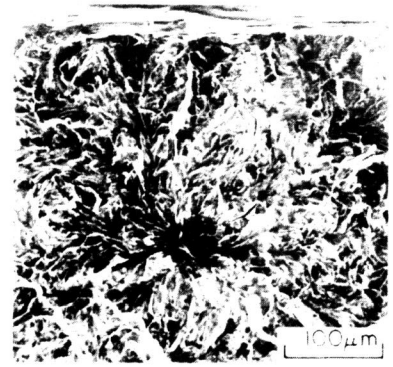

Fig. 4. Cleavage fracture near the notch root (top). Arrow locates possible initiation site.

Isolated sub-notch cracks were observed in the longitudinal sections made on the unbroken ligaments of double-notched specimens, as well as in the sections made on single-notched specimens unloaded prior to final fracture. Figs. 5a and 5b show the typical location and appearance of sub-notch cracks in the unbroken ligament of a double-notched fine pearlitic specimen fractured at room temperature (i.e. at general yield). Fig. 5b shows that the large sub-notch crack illustrated in Fig. 5a consists of four or five pearlite colony-sized cracks, each 4-6 μm in length. The morphology of each colony-sized crack was consistent with the description of shear cracking in pearlite (Miller and Smith, 1970), the schematic for which was illustrated in Fig. 1. Sub-notch cracks of similar appearance were observed in specimens tested at each temperature, although the cracks generally decreased in size with decreasing test temperature (Lewandowski, 1983). In all cases, cracks appeared to initiate in pearlite colonies which were suitably oriented with respect to the maximum longitudinal stress, in the manner described above. Furthermore, good agreement was obtained between the location of the possible initiation sites observed on the fracture surfaces of double-notched specimens (e.g. Fig. 4) and that observed in the longitudinal sections made on the unbroken ligaments of those same specimens (e.g. Fig. 5a). However, the sub-notch cracks were always located closer to the notch than the predicted (Griffiths and Owen, 1971) locations of the maximum longitudinal stress at final fracture (Lewandowski, 1983).

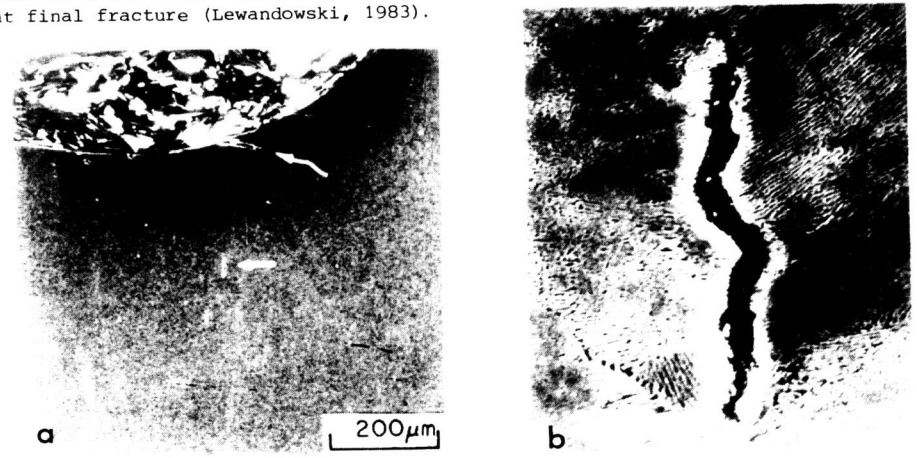

Fig. 5. a) Unetched longitudinal section of bend bar showing sub-notch crack. Straight arrow locates sub-notch crack.

b) Nital-etched sub-notch crack.

Coarse pearlitic specimens exhibited more ductility on their fracture surfaces in comparison to the fine pearlitic specimens. Ductile regions were observed both near the notch root as well as in the overload regions of specimens fractured prior to general yield. Longitudinal sectioning of the unbroken ligaments in double-notched specimens also revealed cracks which appeared to emanate from the notch surface.

DISCUSSION

The critical cleavage fracture stresses reported in the present work were calculated with the aid of a finite-element analysis which assumed only moderate linear work-hardening (Griffiths and Owen, 1971). Although another finite-element analysis (Owen and co-workers, 1973) conducted with linear work-hardening rates ranging from E/120 to E/20 essentially reproduced the Griffiths and Owen (1971) results, work-hardening rates in excess of E/20 produced results different from both slip-line field theory and the Griffiths and Owen (1971) results. The fully pearlitic microstructures tested in the present work exhibited power-law work-hardening at rates in excess of E/120, but less than E/20 (Lewandowski, 1983). While linear work-hardening is a simplification of strain-hardening behaviour, recent finite-element results (Alexander and co-workers, 1984; Knott, 1984) conducted with power-law hardening were not significantly different from the Griffiths and Owen (1971) results, at least for work-hardening exponents up to n = 0.2. Consequently, the present bend bar data will be discussed in light of the Griffiths and Owen (1971) results.

Fine pearlitic specimens which fractured prior to general yield exhibited values for σ_F that were independent of both test temperature and loading rate, consistent with previous results (Knott, 1966a) obtained on mild steel. Furthermore, the ratio of the fracture stresses between the two fine pearlitic microstructures (1900 MPa vs. 1620 MPa, ratio = 1.17) is identical to the ratio of their yield strengths at room temperature (760 MPa vs. 630 MPa, ratio = 1.17) as well as at the lower test temperatures. Since the interlamellar spacing controls yielding in fully pearlitic microsturctures, σ_F increases with decreasing interlamellar spacing and is independent of the prior austenite grain size. These calculations, in combination with the observations of sub-notch cracks, are consistent with Orowan's (1945) proposal that a critical value of tensile stress is required to produce cleavage. However, the sub-notch cracks were always closer to the notch than the predicted (Griffiths and Owen, 1971) location of the maximum longitudinal stress, σ_{yy}, given the location of σ_{yy} at final fracture (Lewandowski, 1983). While sub-notch initiation illustrates the importance of tensile stresses for cleavage fracture in fully pearlitic microstructures, this disagreement in the location of the initiation sites suggests that a more complicated fracture criterion may be required for fully pearlitic microstructures. Although it is possible that sub-notch cracking occurred at loads much lower than the final fracture load, sectioning of bend specimens unloaded at 90% of σ_F failed to reveal any sub-notch cracks (Lewandowski, 1983).

Since the principal strains increase as one proceeds toward the notch root (Griffiths and Owen, 1971), it appears that fracture initiation in the fine pearlitic bend specimens occurred by a strain-assisted process. The morphology of the sub-notch cracks with respect to the microstructure supports such an argument, as sub-notch cracks were observed to occur only in pearlite colonies which were suitably oriented with respect to the maximum longitudinal stress, as shown in Fig. 5b. The available evidence indicates that fracture initiation in the fine pearlitic specimens occurred by a strain-assisted process, while subsequent propagation occurred at a temperature independent value of tensile stress, σ_F, consistent with propagation-controlled cleavage.

Coarse pearlitic specimens, on the other hand, exhibited temperature dependent values for σ_F, although the ratios of σ_F for the two coarse pearlitic microstructures similarly agreed with the ratios of their yield strengths. The presence of more ductility on their fracture surfaces in comparison to fine pearlitic specimens fractured prior to general yield suggests that a critical strain, or stress-strain product, may be necessary to describe cleavage in the coarse pearlitic microstructures. Observations of cracks initiating at the notch in coarse pearlitic specimens fractured prior to general yield (Lewandowski, 1983) further indicate that strain localization at the notch may be a contributing factor toward the observed temperature dependence of σ_F. The possible microstructural reasons for this observed behaviour are presented elsewhere (Lewandowski, 1983; Lewandowski and Thompson, 1984; Porter, Easterling, and Smith, 1978).

CONCLUSIONS

1. The interlamellar spacing controls σ_F for fully pearlitic bend specimens fractured prior to general yield. The prior austenite grain size had no effect on σ_F, although cleavage facet sizes correlated with this microstructural parameter.
2. Fracture initiation in notched bend specimens possessing fine pearlitic microstructures occurs by a strain-assisted process. Subsequent propagation occurs at a temperature independent value of σ_F, consistent with propagation-controlled cleavage fracture.
3. Coarse pearlitic microstructures exhibited temperature dependent values for σ_F, indicating that a critical strain, or stress-strain product, may be necessary to describe cleavage in those microstructures.

ACKNOWLEDGEMENTS

The authors would like to thank J.F. Knott and I.M. Bernstein for fruitful discussions concerning cleavage fracture and fracture of fully pearlitic microstructures. One of the authors (JJL) would also like to thank the Fannie and John Hertz Foundation for the award of a graduate fellowship tenable at C-MU, where this work was conducted. Portions of this work were also supported by the National Science Foundation under grant DMR - 8119540. This manuscript was prepared while one of the authors (JJL) was a NATO Postdoctoral Fellow at the Department of Metallurgy and Materials Science, University of Cambridge, Cambridge, UK.

REFERENCES

Alexander, D. J. (1983). Unpublished research, Carnegie-Mellon University.

Alexander, D. J., J. J. Lewandowski, A. W. Thompson, and I. M. Bernstein (1984). Work-hardening effects on notched bar yielding. Manuscript in preparation.

Burns, K. W. and F. B. Pickering (1964). J.I.S.I., 202, 889-906.

Cottrell, A. W. (1958). Trans. Am. Inst. Min. Metall. Petrol. Engrs., 212, 192-203.

Curry, D. A. (1982). Metal Sci., 16, 435-40.

Curry, D. A. and J. F. Knott (1978). Metal Sci., 12, 511-14.

Green, A. P. and B. B. Hundy (1956). J. Mech. Phys. Sol., 4, 128-44.

Griffiths, J. R. and D. R. J. Owen (1971). J. Mech. Phys. Sol., 19, 419-31.

Hendrickson, J. A., D. S. Wood, and D. S. Clark (1958). Trans. ASM, 50, 656-81.

Hyzak, J. M. and I. M. Bernstein (1976). Met. Trans. A, 7A, 1217-24.

Knott, J. F. (1966a). J.I.S.I., 204, 104-11.

Knott, J. F. (1966b). J.I.S.I., 204, 1014-21.

Knott, J. F. (1984). Personal communication, University of Cambridge.

Kötilainen, H. (1980). Ph.D. Thesis, Technical Research Center of Finland.

Langford, G. (1977). Met. Trans. A, 8A, 861-75.

Lewandowski, J. J. (1983). Hydrogen effects on cleavage fracture in fully pearlitic 1080 steel. Ph.D. Thesis, Carnegie-Mellon University.

Lewandowski, J. J. and A. W. Thompson (1984). Manuscript in preparation.

Lindley, T. C., G. Oates, and C. E. Richards (1970). Acta Met., 18, 1127-36.

McMahon, C. J. and M. Cohen (1965). Acta Met., 13, 591-614.

Miller, L. E. and G. C. Smith (1970). J.I.S.I., 208, 998-1005.

Orowan, E. (1945). Trans. Inst. Engrs. Shipbuilders Scot., 89, 165-215.

Owen, D. R. J., G. C. Nayak, A. P. Kfouri, and J. R. Griffiths (1973). Int. J. Num. Meth. Eng., 6, 63-73.

Park, Y. J. and I. M. Bernstein (1979). Met. Trans. A, 10A, 1653-64.

Pepe, J. J. (1973). Met. Trans., 4, 2455-60.

Porter, D. A., I. E. Easterling, and G. D. W. Smith (1978). Acta Met., 26, 1405-22.

Smith, E. (1966). Proc. Conf. Phys. Basis of Yield and Fracture, Inst. Phys. Soc., Oxford, 36-46.

Stroh, A. N. (1954). Proc. Roy. Soc., A223, 404-14.